

# **MBE growth of HgCdTe on GaSb substrates for application in next generation infrared detectors**

R. Gu, J. Antoszewski, W. Lei, I. Madni, G. Umana-Membreno, L. Faraone

School of Electrical, Electronic and Computer Engineering, The University  
of Western Australia, Crawley, 6009, WA, Australia

## **Abstract**

HgCdTe has dominated the high performance end of the IR detector market for decades. At present, the cost to fabricate HgCdTe based advanced infrared devices is relatively high. One approach to address this problem is to use cost effective alternative substrate, mainly Si and GaAs. Recently, GaSb has emerged as a new alternative with better lattice matching. In this paper, recent progress in molecular beam epitaxial (MBE) growth of HgCdTe infrared material at UWA is reported. HgCdTe has been grown on GaSb substrates by MBE, and has shown a lower Etch Pit Density (EPD) and higher minority carrier lifetime in comparison to other alternative substrates. This result makes GaSb an interesting and promising alternative substrate material for HgCdTe epitaxy.

**Key words:** A3. MBE, HgCdTe, alternative substrate, GaSb, EPD, lifetime

## **Introduction**

Currently,  $\text{Cd}_{0.96}\text{Zn}_{0.04}\text{Te}$  (CZT) substrates are the preferred substrates for fabricating high performance HgCdTe infrared focal plane arrays (IRFPAs) due to their nearly zero lattice mismatch with HgCdTe. However, they suffer some serious limitations such as small wafer size, high cost, relatively poor quality, low mechanical strength, and low thermal conductivity. Therefore, in recent years researchers have trialed alternative substrates in order to overcome the limitations suffered by CZT. Three main alternative substrates have been studied, e.g. Si [1-3], Ge [4-5] and GaAs [6-8], and mid-wave infrared HgCdTe detectors grown on these alternative substrates have demonstrated similar performance to those grown on CZT. However, lattice and thermal mismatch has become increasingly important due to the industry trend towards smaller pixel size and larger detector arrays. Stress due to lattice and thermal mismatch is an important issue in epitaxially-grown semiconductors. It leads to mismatch defects such as dislocations which are known to be the source of effective recombination and have impact

on yield and electro-optical properties of the device [9-10]. Due to the large lattice mismatch between HgCdTe and the alternative substrates, a large dislocation density is observed, which reduces the performance of HgCdTe infrared detectors. Therefore, new alternative substrates are needed for growth of high quality HgCdTe materials. [11-12]

Figure 1 shows the lattice constant and coefficient of thermal expansion (CTE) of several potential alternative substrates. [13] The lattice constant mismatch between GaSb and HgCdTe is much smaller than that of Si, Ge and GaAs. In addition, the CTE mismatch of GaSb/HgCdTe is comparable to that of Ge/HgCdTe and GaAs/HgCdTe and much smaller than Si/HgCdTe. Therefore, in principle, HgCdTe grown on GaSb substrates should result in lower dislocation densities than if grown on other alternative substrates.

### **Experimental Growth and Characterization**

To evaluate the feasibility of GaSb alternative substrates for growing high quality materials, HgCdTe has been grown using a Riber 32P MBE system. For comparison, HgCdTe materials have also been grown on GaAs and CdZnTe substrates (structures illustrated in Figure 2). In the case of GaAs substrates, due to higher lattice mismatch than GaSb,

a low temperature ZnTe nucleation technique was introduced to prevent twin generation (Fig. 2c). An non-optimized HgCdTe/CdTe/GaAs structure was also grown for comparison (Fig. 2b).

Both GaAs and GaSb 211(B) substrates were epitaxy-ready from Wafer Technology Ltd. The CdZnTe substrates were etched in 0.5% Bromine-Methanol solution to remove any oxide layer on the surface, and then rinsed in methanol followed by deionized (DI) water. All substrates were pre-baked at a temperature of 150°C before thermal cleaning. After thermal cleaning, a reflection high-energy electron diffraction (RHEED) system was used to check the surface quality before sample growth. During growth, the Rheed system showed a clean and smooth growth front on GaSb, CZT and optimized GaAs substrates.

HgCdTe composition and thickness of each layer was extracted using the Fourier transform infrared spectroscopy (FTIR) technique. It showed that all four samples had comparable parameters (Tab.3). The FWHM of XRD rocking curve for HgCdTe on CdZnTe substrate is much narrower than that on GaSb and GaAs substrates, due to higher lattice mismatch for these two alternative substrate materials.

The EPD experiment was performed by wet etching using Chen's recipe ( $\text{H}_2\text{O} : \text{HCL} : \text{HNO}_3 : \text{K}_2\text{CR}_2\text{O}_7 = 80\text{ml} : 10\text{ml} : 20\text{ml} : 8\text{g}$ ) for 3mins

[14], followed by rinsing with DI water and drying with N<sub>2</sub> before checking under a 1000x microscope. The EPD on HgCdTe/CdTe/GaSb was much lower than that on GaAs substrate (Figure 3). In spite of the fact that the epitaxy process on GaSb has not yet been optimized, the EPD showed that HgCdTe grown on GaSb substrates resulted in a considerable decrease of native dislocations in HgCdTe.

In HgCdTe materials, the minority carrier lifetime is a function of material x-value, defect types and density, conductivity type, and carrier concentration. For a certain x-value and carrier concentration, the lifetime will roughly reflect the defect density in the HgCdTe material. Minority carrier lifetimes were measured using the photoconductive decay technique. Note that no post-growth annealing or surface passivation layer was applied on any of the samples. To avoid sweep-out effects, the sample biasing was kept low (300 mV), and all photoconductive decay curves were fitted exponentially to obtain the minority carrier lifetimes.

Several different recombination mechanisms determine the photo-generated minority carrier lifetime in HgCdTe, such as Auger, radiative, and Shockley-Read-Hall mechanisms, which have been discussed extensively in the literature [15–21]. The extracted lifetime

values, from the temperature dependent photoconductive decay measurement results, are illustrated in Figure 4. HgCdTe grown on GaSb substrates has a lifetime of around 900ns at 77K. The lifetime results showed a similar trend of that on EPD, that HgCdTe grown on GaSb has a higher quality than that on GaAs.

Figure 5 shows the experimental EPD and minority carrier lifetime in mid-wave infrared HgCdTe layers grown on different substrates vs lattice mismatch of HgCdTe and substrates. Note that the EPD of HgCdTe grown on different substrates is taken from the literature [22-27]. The curve plotted in Figure 6 is only for eye guidance and easy comparison, and does not have physical meaning.

It is observed that the EPD decreases and lifetime increases with reducing lattice mismatch between HgCdTe and the substrate. The EPD measured on HgCdTe/CdTe/GaSb samples was significantly lower in comparison to the values measured on un-optimized GaAs substrates, and being a factor of 3 lower than on the GaAs sample with an optimized low-temperature ZnTe nucleation layer. The results from lifetime measurement also consistent with these results. Considering that the HgCdTe epitaxial growth process on GaSb has yet to be optimized, the lower EPD and higher lifetime values for HgCdTe grown on GaSb

substrates are likely to be directly linked to a considerable decrease in native dislocation density in the HgCdTe layer, suggesting that this approach has potential future application for producing high performance devices and high-yield IRFPAs.

## **Conclusion**

In this work, GaSb has been investigated as a new alternative substrate for the epitaxial growth of HgCdTe infrared materials. Results obtained for GaSb demonstrate its potential as an alternative substrate for HgCdTe/CdTe growth. MBE growth of HgCdTe/CdTe on GaSb and GaAs has demonstrated that the HgCdTe material quality on GaSb is comparable to or slightly better than that on GaAs substrates, a growth technology that has been developed for decades. Further, XRD, EPD and lifetime characterization of the HgCdTe epitaxial layers indicate that fewer dislocations are generated at the GaSb/CdTe/HgCdTe interface in comparison to GaAs/CdTe/HgCdTe. The experimental observations and simulation analysis clearly indicate that GaSb shows great promise for potential application in this area. In future work, the MBE growth parameters of HgCdTe/CdTe/GaSb structures will be optimized

experimentally in an attempt to improve on the preliminary results presented in this paper.

## ACKNOWLEDGEMENTS

This work was supported by the Australian Research Council (FT130101708, DP150104839), and Universities Australia DADD German Research Cooperation program (2014-2015), and UWA Research Collaboration Awards (2016). Facilities used in this work are supported by the WA node of Australian National Fabrication Facility (ANFF).

## REFERENCES

- [1] T. J. de Lyon, J. E. Jensen, M. D. Gorwitz, C. A. Cockrum, S. M. Johnson, G. M. Venzor, "MBE growth of HgCdTe on silicon substrates for large-area infrared focal plane arrays: A review of recent progress", *J. Electronic Materials*, 1999, 28(6): 705
- [2] G. Brill, S. Velicu, P. Boieriu, Y. Chen, N. K. Dhar, T. S. Lee, Y. Selamet, S. Sivananthan, "MBE growth and device processing of MWIR HgCdTe on large area Si substrates", *J. Electronic Materials*, 2001, 30(6): 717
- [3] J. B. Varesi, R. E. Bornfreund, A. C. Childs, W. A. Radford, K. D. Maranowski, J. M. Peterson, S. M. Johnson, L. M. Giegerich, T. J. de Lyon, J. E. Jensen, "Fabrication of high-performance large-format MWIR focal plane arrays from MBE-grown HgCdTe on 4" silicon substrates", *J. Electronic Materials*, 2001, 30(6): 566
- [4] P. Ferret, J. P. Zanatta, R. Hamelin, S. Cremer, A. Million, M. Wolny, G. Destefanis, "Status of the MBE technology at leti LIR for the manufacturing of HgCdTe focal plane arrays", *J. Electronic Materials*, 2000, 29(6): 641
- [5] J. P. Zanatta, G. Badano, P. Ballet, C. Largeron, J. Baylet, O. Gravrand, J. Rothman, P. Castelein, J. P. Chamonal, A. Million, G. Destefanis, S. Mibord, E. Brochier, P. Costa, "Molecular beam epitaxy growth of HgCdTe on Ge for third-generation infrared detectors", *J. Electronic Materials*, 2006, 35(6): 1231



- [6] L. He, L. Chen, Y. Wu, X.L. Fu, Y.Z. Wang, J. Wu, M.F. Yu, J.R. Yang, R.J. Ding, X.N. Hu, Y.J. Li, Q.Y. Zhang, "MBE HgCdTe on Si and GaAs substrates", *J. Crystal Growth*, 2007, 301–302: 268–272
- [7] R.N. Jacobs, C. Nozaki, L.A. Almeida, M. Jaime-Vasquez, C. Lennon, J.K. Markunas, D. Benson, P. Smith, W.F. Zhao, D.J. Smith, C. Billman, J. Arias, J. Pellegrino, "Development of MBE II–VI Epilayers on GaAs(211)B", *J. Electronic Materials*. 2012, 41(10): 2707
- [8] J.D. Benson, L.O. Bubulac, P.J. Smith, R.N. Jacobs, J.K. Markunas, M. Jaime-Vasquez, L.A. Almeida, A. Stoltz, J.M. Arias, G. Brill, Y. Chen, P.S. Wijewarnasuriya, S. Farrell, U. Lee, "Growth and Analysis of HgCdTe on Alternate Substrates", *J. Electronic Materials*, 2012, 41(10): 2971.
- [9] W. Lei, J. Antoszewski, and L. Faraone, *Appl. Phys. Rev.*, 2, 041303 (2015).
- [10] R. Gu, W. Lei, J. Antoszewski, I. Madni, G. Umana-Membreno, L. Faraone, "Recent progress in MBE grown HgCdTe materials and devices at UWA", *Proc. SPIE* 9819, 98191Z (2016); doi:10.1117/12.2222997.
- [11] W. Lei, R. J. Gu, J. Antoszewski, J. Dell, L. Faraone, "GaSb: A New Alternative Substrate for Epitaxial Growth of HgCdTe", *J. Electronic Materials*, 2014, 43(8): 2788-2794
- [12] W. Lei, R.J. Gu, J. Antoszewski, J. Dell, G. Neusser, M. Sieger, B. Mizaiakoff, and L. Faraone, "MBE Growth of Mid-wave Infrared HgCdTe Layers on GaSb Alternative Substrates", *J Electron Mater.*, 44, 3180 (2015).
- [13] R. Gu, W. Lei, J. Antoszewski, L. Faraone, "Investigation of Substrate Effects on Interface Strain and Defect Generation in MBE-Grown HgCdTe", *J Electronic Materials*, (2016), doi:10.1007/s11664-016-4558-6
- [14] J.S. Chen, US patent, (No.4, 897, 1990), p152
- [15] M. A. Kinch, M. J. Brau, and A. Simmons, "Recombination mechanisms in 8–14- $\mu\text{m}$  HgCdTe," *J. Appl. Phys.* 72, 4261 (1992).
- [16] J. S. Blakemore, *Semiconductor Statistics* (Pergaman, New York, 1962), p. 196.
- [17] I. M. Baker, F. A. Capocci, D. E. Charlton, and J. T. M. Wotherspoon, "Recombination in cadmium mercury telluride photodetectors," *Solid-State Electron.* 21, 1475 (1978).
- [18] M. Y. Pines and O. M. Stafsudd, "Recombination process in intrinsic semiconductors using impact ionization capture cross sections in indium antimonide and mercury cadmium telluride," *Infrared Phys.* 20, 73 (1980).
- [19] W. Shockley and W. T. Read, "Statistics of the recombinations of holes and electrons," *Phys. Rev.* 87, 835 (1952).
- [20] C. T. Sah and W. Shockley, "Electron-hole recombination statistics in semiconductors through flaws with many charge conditions," *Phys. Rev.* 109, 1103 (1958)
- [21] I. Madni, G. A. Umana-Membreno, W. Lei, R. Gu, J. Antoszewski, and L. Faraone, "Minority carrier lifetime in iodine-doped molecular beam epitaxy-grown HgCdTe", *Applied Physics Letters* 107, 182107 (2015); doi: 10.1063/1.4935154
- [22] J.D. Benson, L.O. Bubulac, P.J. Smith, R.N. Jacobs, J.K. Markunas, M. Jaime-Vasquez, L.A. Almeida, A.J. Stoltz, P.S. Wijewarnasuriya, G. Brill, Y. Chen, U. Lee, M.F. Vilela, J. Peterson, S.M. Johnson, D.D. Lofgreen, D. Rhiger, E.A. Patten, and P.M. Goetz. "Characterization of Dislocations in (112) B HgCdTe/CdTe/Si ", *J Electron Mater.*, 39(7): 1080-1086 (2010).

- [23] M. Carmody, A. Yulius, D. Edwall, D. Lee, E. Piquette, R. Jacobs, D. Benson, A. Stoltz, J. Markunas, A. Almeida, and J. Arias. "Recent progress in MBE growth of CdTe and HgCdTe on (211) B GaAs substrates", *J Electron Mater.*, 41(10): 2719-2724 (2012).
- [24] M. Carmody, J.G. Pasko, D. Edwall, R. Bailey, J. Arias, M. Groenert, L.A. Almeida, J.H. Dinan, Y. Chen, G. Brill, and N.K. Dhar. "LWIR HgCdTe on Si detector performance and analysis", *J Electron Mater.*, 35(6): 1417-1422 (2006).
- [25] D. Edwall, E. Piquette, J. Ellsworth, J. Arias, C.H. Swartz, L. Bai, R.P. Tompkins, N.C. Giles, T.H. Myers, and M. Berding. "Molecular beam epitaxy growth of high-quality arsenic-doped HgCdTe", *J Electron Mater.*, 33(6): 752-756 (2004).
- [26] M. Carmody, J.G. Pasko, D. Edwall, R. Bailey, J. Arias, S. Cabelli, J. Bajaj, L.A. Almeida, J.H. Dinan, M. Groenert, A.J. Stoltz, Y. Chen, G. Brill, and N.K. Dhar. "Molecular beam epitaxy grown long wavelength infrared HgCdTe on Si detector performance", *J Electron Mater.*, 34(6): 832-838 (2005).
- [27] S.M. Johnson, A.A. Buell, M.F. Vilela, J.M. Peterson, J.B. Varesi, M.D. Newton, G.M. Venzor, R.E. Bornfreund, W.A. Radford, E.P.G. Smith, J.P. Rosbeck, T.J. de Lyon, J.E. Jensen, and V. Nathan. "HgCdTe/Si materials for long wavelength infrared detectors", *J Electron Mater.*, 33(6): 526-530 (2004).

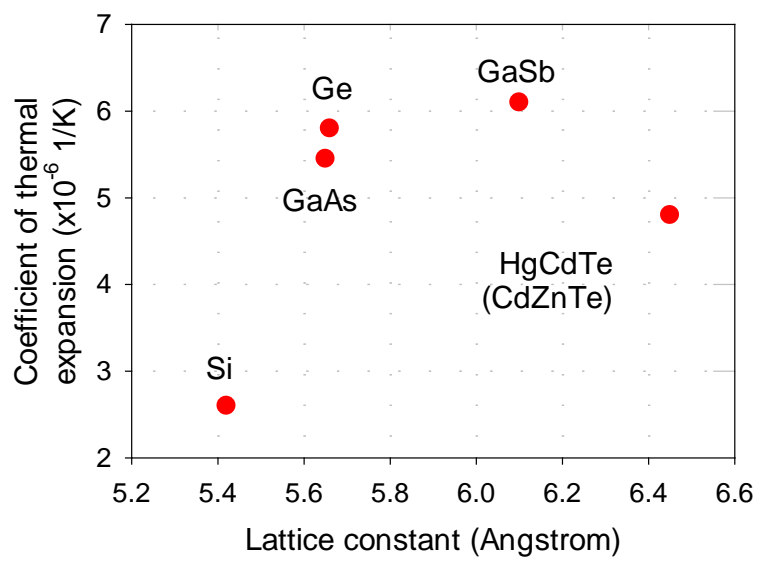


Fig. 1. Lattice and CTE mismatch between HgCdTe and substrates

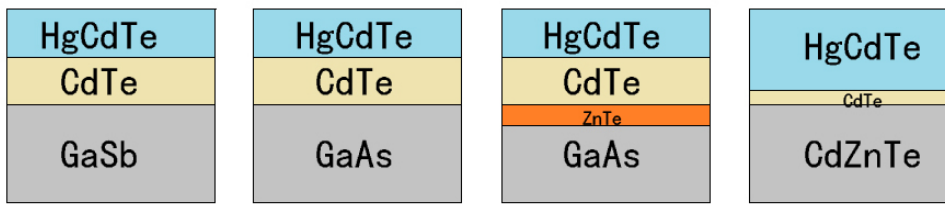
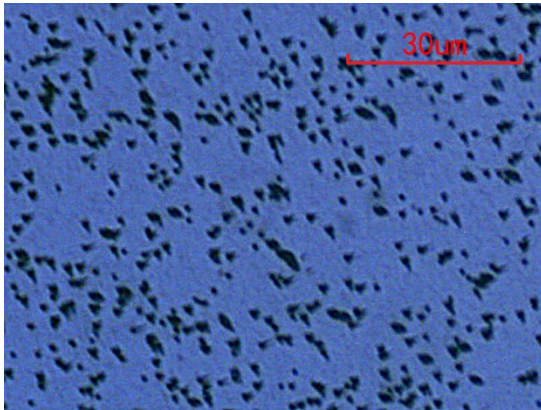
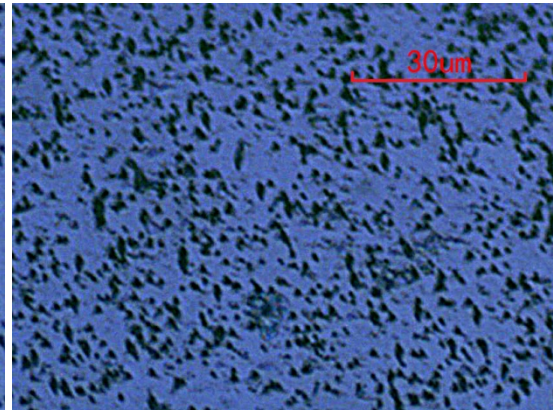


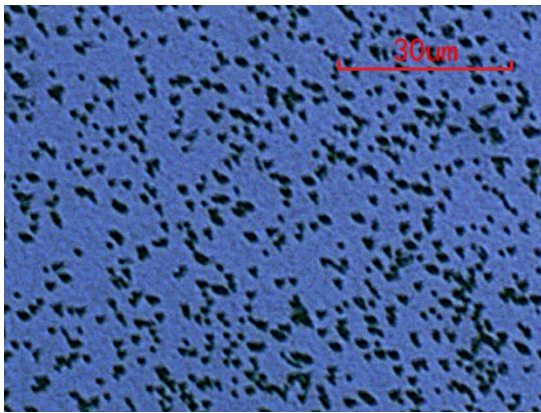
Fig 2 Growth structure for different substrates. (a) GaSb substrate with 5 $\mu$ m buffer layer. (b) GaAs substrate with the same structure of GaSb for compare (c) GaAs substrate with nucleation technology and 5 $\mu$ m buffer (d) CZT substrate with 50nm thin buffer layer



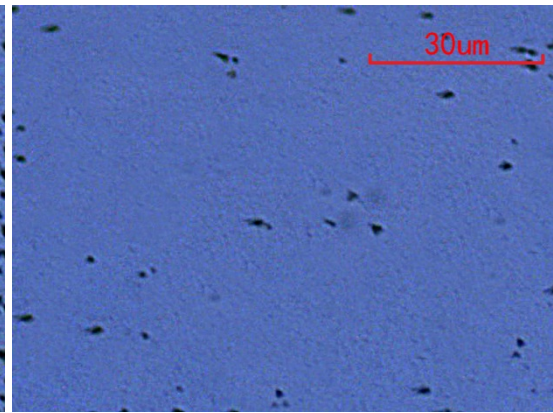
(a) GaSbMCT-1 EPD= $2 \times 10^6 \text{ cm}^{-2}$



(b) GaAsMCT w/o ZnTe EPD= $2 \times 10^7 \text{ cm}^{-2}$



(c) GaAsMCT with ZnTe EPD= $6 \times 10^6 \text{ cm}^{-2}$



(d) CdZnTeMCT-1 EPD= $2 \times 10^4 \text{ cm}^{-2}$

Fig 3 FPD on all substrates

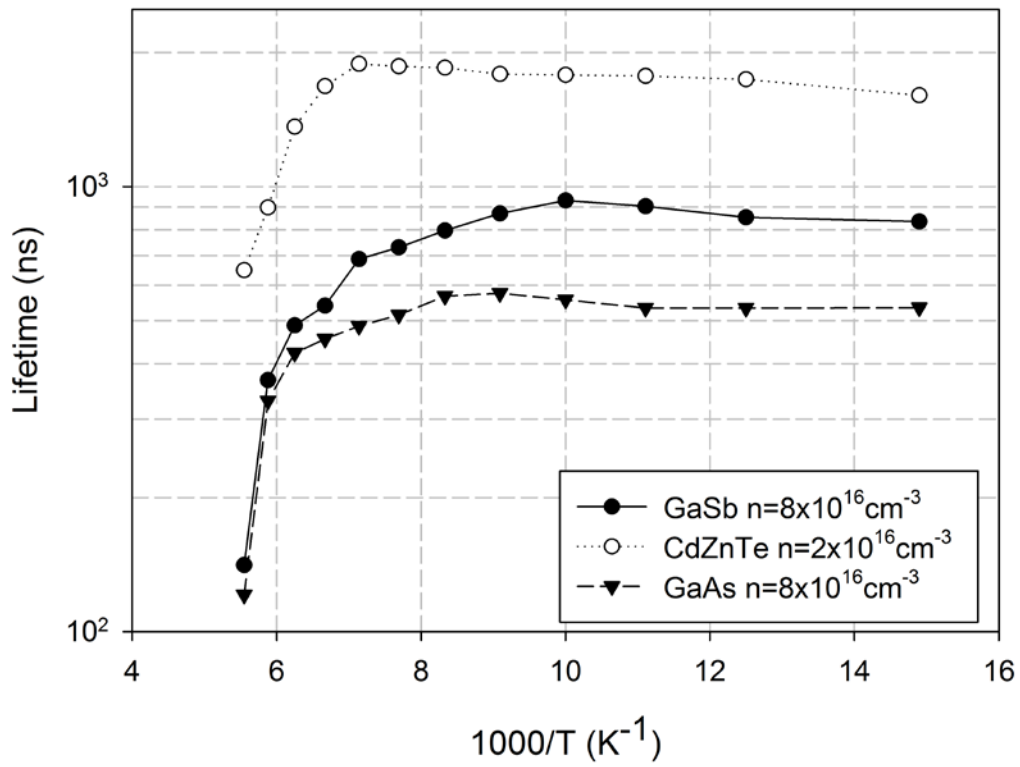


Fig. 4 Minority carrier lifetime for HgCdTe on GaSb, CdZnTe and GaAs, as a function of temperature.

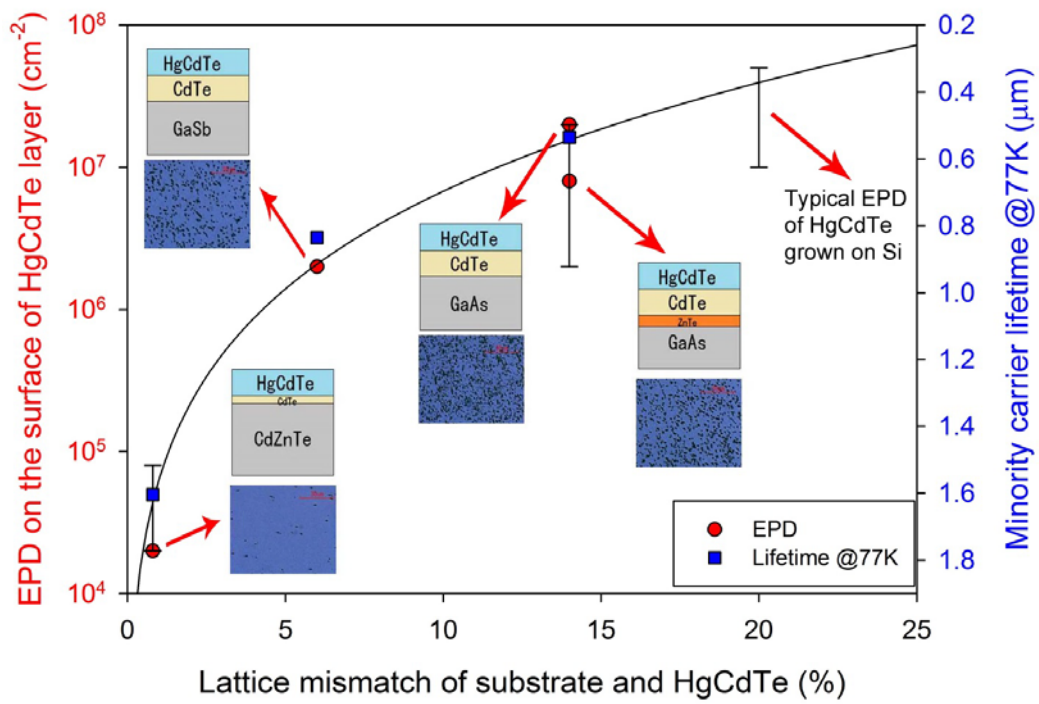


Fig 5 Relationship between modelled strain at substrate/CdTe buffer interface and measured EPD / lifetime on HgCdTe. The error bars represent the typical EPD range of as-grown HgCdTe ( $x \sim 0.3$ ) on different substrates from Refs.<sup>22-27</sup>

Table I. Material parameters for each layer, composition and thickness data extracted from FTIR.

Sample No.	Substrate	Nucleation Layer	Thickness of CdTe (um)	Thickness of HgCdTe (um)	x-value	XRD FWHM (arcsec)	EPD ( $\times 10^4 \text{cm}^{-2}$ )
a	GaSb	N	5.3	5.7	0.325	122	200
b	GaAs	N	5.6	5.6	0.318	191	2000
c	GaAs	Y	5.7	5.1	0.322	98	600
d	CdZnTe	N	10E-3	4.7	0.298	54	2